

JOM 23877

An NMR investigation of 1,2-metallotropic shifts in transition metal complexes of benzo[*c*]cinnoline and pyridazines

Edward W. Abel, Elizabeth S. Blackwall, Keith G. Orrell and Vladimir Šik

Department of Chemistry, University of Exeter, Devon EX4 4QD (UK)

(Received April 22, 1993)

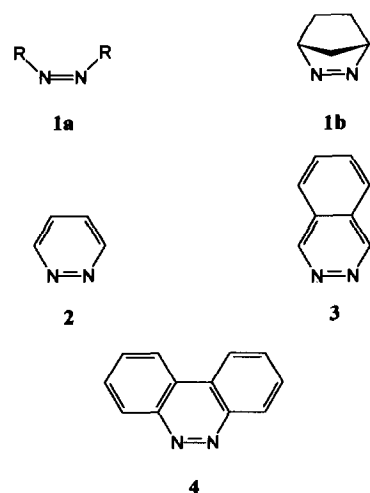
Abstract

Complexes of types $[\text{W}(\text{CO})_5\text{L}]$, $[\text{cis-Rh}(\text{CO})_2\text{ClL}]$ ($\text{L} = \text{benzo}[c]\text{cinnoline}$) and $[\text{W}(\text{CO})_5\text{L}']$ ($\text{L}' = \text{pyridazine}$, 3-methylpyridazine, and 4-methylpyridazine) have been synthesized and shown to exhibit, in organic solvents, intramolecular metal–nitrogen 1,2-fluxional shifts, which have been quantitatively studied by 1D bandshape analysis and 2D-EXSY NMR experiments. Energy barriers for the metallotropic shifts in the pyridazine complexes are *ca.* 20 kJ mol^{-1} higher than in the benzo[*c*]cinnoline complexes. These differences are discussed in terms of the ground state and likely transition state species for this fluxional process.

Key words: Tungsten; Rhodium; Pyridazine; Nuclear magnetic resonance; Metallotropic shift

1. Introduction

Diazene ligands form a wide range of complexes with transition metal moieties. Where the nitrogen



donors are contiguous, the possibility of 1,2-metallotropic shifts exists and several cases have been identified. Previous studies of 1,2-metal–nitrogen shifts have included transition metal complexes of azo compounds (**1a**, **b**) [1–5], pyridazine (pydz) (**2**) [6], phthalazine (phth) (**3**) [7,8] and benzo[*c*]cinnoline (bzc) (**4**) [3,9]. The two main physical methods employed were electronic absorption/emission spectrophotometry and variable temperature NMR spectroscopy. Both techniques clearly established the existence of these fluxional shifts but very little quantitative data pertaining to them have been reported probably on account of the complexity of the spectra in most cases. Modern techniques of dynamic NMR spectroscopy [10] such as total bandshape analysis and two-dimensional exchange spectroscopy (2D-EXSY) [11], have the potential to provide reliable rate and activation energy data for these shifts, and this paper shows how these techniques have been applied to transition metal complexes of pyridazines and benzo[*c*]cinnoline, namely $[\text{W}(\text{CO})_5(\text{bzc})]$, $[\text{cis-Rh}(\text{CO})_2\text{Cl}(\text{bzc})]$, and $[\text{W}(\text{CO})_5\text{L}']$ ($\text{L}' = \text{pydz}$, 3-methylpydz and 4-methylpydz). The resulting energy data are discussed in terms of the factors influencing the 1,2-metal–nitrogen shift and, in particular, the probable electronic nature of the transition state species.

Correspondence to: Dr. K.G. Orrell.

2. Experimental details

2.1. General

All preparations involving air-sensitive materials were carried out under dry, oxygen-free nitrogen by standard Schlenk techniques [12]. All solvents were freshly distilled under nitrogen and dried as follows, benzene and tetrahydrofuran (THF) on sodium diphenyl ketyl, hexane and light petroleum (b.p. 40–60°C) on sodium wire, and dichloromethane on calcium hydride.

Melting points were taken on a digital Gallenkamp apparatus, and were uncorrected. Elemental analyses were carried out by Butterworth Laboratories Ltd., Teddington, Middlesex. Infrared spectra of CH₂Cl₂ solutions of the complexes were recorded on a Perkin Elmer Model 881 spectrometer using matched CaF₂ solution cells.

¹H NMR spectra were recorded on a Bruker AM 250 spectrometer operating at 250.13 MHz. Chemical shifts are quoted relative to internal Me₄Si. Samples were measured as solutions in CDCl₃, C₆D₆ or (CDCl₂)₂. NMR probe temperatures were varied using the standard B-VT 1000 accessory with the calibration being checked against a Comark digital thermometer. Quoted temperatures are considered accurate to ± 1°C. NMR bandshape analyses were performed with the authors' version of the standard DNMR3 program [13]. ¹H 2D-EXSY NMR experiments were obtained with the Bruker automation program NOESYPH with the pulse sequence D1–90°–D0–90°–D9–90°–FID. The relaxation delay D1 were set at 2.0 s and the evolution time D0 had an initial value of 3 × 10⁻⁶ s. The mixing time D9 (τ_m) was varied between 0.1 and 2.5 s according to the complex and the measurement temperature.

The sizes of the frequency domains F1 and F2 were 256 words. The spectral width was typically 200 Hz and the number of pulse sequences per experiment was in the range 16–64. Data processing incorporated an exponential window function with a line broadening of 0.5 Hz in both frequency dimensions. Rate data were calculated from the 2D-EXSY contour plots using our D2DNMR program [14].

2.2. Synthesis of compounds

The general method of preparing the metal pentacarbonyl complexes involved preparing the photochemically generated species [M(CO)₅(THF)] (M = Cr, Mo, W) [15] and then stirring it with the appropriate ligand in THF, with only the reaction time varying between complexes. Progress of the reactions, which were carried out in the dark, was monitored by IR spectroscopy. The synthesis of [W(CO)₅(bzc)] is given as an illustrative example [16].

To a solution of [W(CO)₅THF] (0.78 g, 2.0 mmol) in THF (80 cm³), the ligand bzc (0.36 g, 2.0 mmol) in THF (20 cm³) was added dropwise and the solution stirred at room temperature for 24 h. The solvent was removed under vacuum to yield a crude product, which was purified by recrystallization from CH₂Cl₂/hexane (1:1) at 0°C and then washed with cold hexane to give red needle-like crystals (0.4 g, 39%).

The complexes [W(CO)₅(pydz)], [W(CO)₅(3-Mepydz)] and [W(CO)₅(4-Mepydz)] were prepared analogously [17]; the reactions were for 8 h at room temperature.

The complex [*cis*-Rh(CO)₂Cl(bzc)] was prepared by the published method [18].

Analytical and characterization data for all the complexes are given in Table 1.

TABLE 1. Analytical and characterization data for transition metal diazene complexes

Complex	Yield ^a (%)	Colour	M.P (°C)	ν(CO) ^b (cm ⁻¹)		Analytical data					
						Found (%)			Calculated (%)		
						C	H	N	C	H	N
[W(CO) ₅ (bzc)]	39	Red crystals	125–135(d) ^c	2070	1920	40.3	1.7	5.6	40.5	1.6	5.6
[<i>cis</i> -Rh(CO) ₂ Cl(bzc)]	44	Yellow crystals	129	2090	2015	44.6	2.3	7.3	44.9	2.1	7.5
[W(CO) ₅ (pydz)]	35	Orange powder		2068	1921	27.3	1.3	6.8	26.8	1.0	6.9
[W(CO) ₅ (3-Mepydz)]	34	Yellow powder	117(d)	2069	1919	28.8	1.5	6.7	28.8	1.5	6.7
[W(CO) ₅ (4-Mepydz)]	30	Orange crystals	94–96(d)	2071	1920	28.7	1.6	6.2	28.7	1.5	6.7

^a Relative to [W(CO)₆]. ^b IR spectra recorded in CH₂Cl₂ solutions. ^c (d), decomposition.

3. Results

3.1. Benzo[*c*]cinnoline complexes

Earlier NMR studies on $[\text{W}(\text{CO})_5(\text{bzc})]$ [3,9] and other $[\text{M}(\text{CO})_5(\text{diazene})]$ complexes utilized ^{13}C spectra of these species in view of the relative ease of line assignments. The total bandshape analyses we wished to pursue are more accurately applied to ^1H spectra in view of the more favourable chemical shift range and greater intensity of ^1H signals. Complete assignments of the ^1H spectra of bzc and its complexes were therefore attempted prior to any dynamic NMR (DNMR) analysis.

The 250 MHz ^1H spectrum of bzc in CDCl_3 consisted of a second-order ABCD spectrum with hydrogens C and D having almost identical chemical shifts. A spectrum in C_6D_6 (Fig. 1) gave a more favourable chemical shifts dispersion and the spectrum was fully analysed by iterative fitting using the standard LAOCN3 program [19]. Spectral parameters are given in Table 2. Room temperature spectra of all three complexes $[\text{M}(\text{CO})_5(\text{bzc})]$ ($\text{M} = \text{Cr}, \text{Mo}, \text{W}$) were recorded in CDCl_3 but the spectra of the $\text{M} = \text{Cr}$ and Mo complexes indicated fairly rapid decomposition with the formation of paramagnetic species which caused considerable broadening of all spectral lines. The tungsten complex, however, was more stable and this was submitted to a full variable temperature NMR analysis with spectra being recorded up to 323 K. Some slight decomposition

was apparent but this did not detract from the DNMR analysis. The 1,2-fluxional shift (Fig. 2) was clearly apparent in the ambient temperature spectra and cooling to *ca.* -50°C (223 K) was required to produce a well resolved "static" spectrum (Fig. 3). This consisted of eight chemically shifted ^1H signals with considerable overlap between some of them. The highest frequency signal was assigned to proton A on account of its large high frequency coordination shift. The corresponding signal in the other ring, due to proton E, was partially obscured by the intense doublet due to the protons B and F which had almost identical shifts. The remaining signals C, D, G and H were less straightforwardly assigned. The assignments given in Table 2 and Fig. 2 were based on the best theoretical fittings for this region.

On warming the CDCl_3 solution of the complex, the spectrum changed as shown in Fig. 3. These changes are clearly the result of the 1,2-fluxional shift causing a pair-wise exchange of all eight ring hydrogens. Since no scalar coupling was detected between hydrogens of different aromatic rings, the exchange process can be accurately described as exchange between two configurations of four spins, namely $\text{ABCD} \rightleftharpoons \text{EFGH}$ (Fig. 2). The DNMR3 program was used for this spin problem and the fittings shown in Fig. 3. The major spectral changes were associated with the exchange of the A and E hydrogens, and emphasis was placed on the accuracy of fitting this part of the spectrum. The best-fit

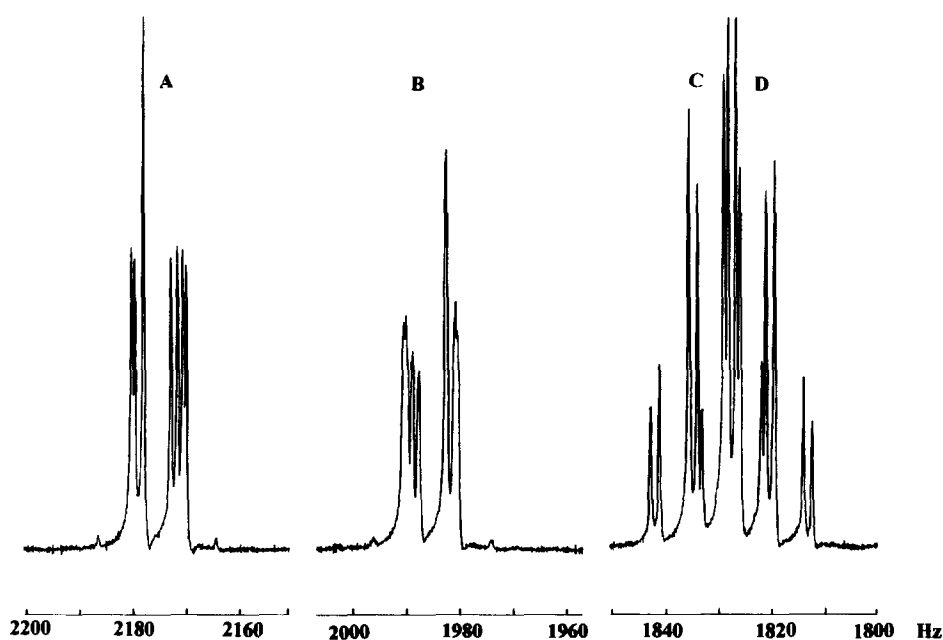


Fig. 1. ^1H NMR spectrum (250.13 MHz) of benzo[*c*]cinnoline in C_6D_6 solvent.

TABLE 2. ^1H NMR data for benzo[*c*]cinnoline (bzc) and its complexes $[\text{M}(\text{CO})_5(\text{bzc})]$ ($\text{M} = \text{Cr}, \text{Mo}, \text{W}$) and $[\text{Rh}(\text{CO})_2\text{Cl}(\text{bzc})]$

Compound	Tem- pera- ture (K)	Solvent	Hydrogen shifts, δ^a										
			A	B	C	D	E	F	G	H			
bzc	303	CDCl_3	8.74	8.55	7.89	7.89							
		C_6D_6	8.70	7.94	7.33	7.28							
$[\text{Cr}(\text{CO})_5(\text{bzc})]$	303	CDCl_3	8.9	8.6	8.0	8.0	8.9	8.6	8.0	8.0			
$[\text{Mo}(\text{CO})_5(\text{bzc})]$	303	CDCl_3	8.88	8.61	8.02	8.00	8.88	8.61	7.94	8.05			
$[\text{W}(\text{CO})_5(\text{bzc})]$	303	CDCl_3	8.90	8.64	8.04	8.02	8.90	8.62	7.99	8.06			
	223	CDCl_3	9.08	8.64	8.08	8.06	8.68	8.64	8.03	7.97			
$[\text{cis-Rh}(\text{CO})_2\text{Cl}(\text{bzc})]$	253	CDCl_3	9.44	8.56	7.91	7.89	8.59	8.56	7.86	7.94			

Compound	Tem- pera- ture (K)	Solvent	Coupling constants J (Hz)											
			AB	AC	AD	BC	BD	CD	EF	EG	EH	FG	FH	GH
bzc	303	CDCl_3	0.61	8.47	1.15	1.45	8.15	7.04						
$[\text{W}(\text{CO})_5(\text{bzc})]$	303	CDCl_3	0.6	8.5	1.2	1.5	8.2	7.0	0.6	9.5	1.2	1.5	8.2	7.0
$[\text{cis-Rh}(\text{CO})_2\text{Cl}(\text{bzc})]$	303	CDCl_3	^b	8.9	2.5	^b	8.5	^b	^b	7.8	2.2	^b	8.5	^b

^a Relative to int. Me_4Si . ^b Exchange broadening prevented these values from being measured.

rate constants for the process are shown in Fig. 3 and these enabled the Eyring activation energy parameters to be calculated (Table 3).

Similar variable temperature studies were carried out on the complex $[\text{cis-Rh}(\text{CO})_2\text{Cl}(\text{bzc})]$. In this case, a spectrum of the "static" complex was achieved at $ca -20^\circ\text{C}$ (253 K), and the signal due to hydrogen E was now quite separate from the B/F signals. Warming this complex led to the expected spectral changes, with the fluxional process being fast on the NMR timescale at 50°C . Bandshape fittings were performed on the A and E proton signals and rate constants based on 11 fittings in the temperature range -10°C to 50°C gave reliable activation energy data (Table 3).

3.2. Pyridazine and methylpyridazine complexes

All three complexes $[\text{W}(\text{CO})_5\text{L}]$ ($\text{L} = \text{pydz}$, 3-Mepydz, and 4-Mepydz) exhibited 1,2 tungsten–nitrogen shifts in CDCl_3 solution. The shift in the unsubstituted pydz complex causes exchange between identical species whereas in the two methyl-substituted pydz complexes this linkage isomerization exchanges chemically distinct forms which have differing solution populations. This is particularly evident in the 3-Mepydz

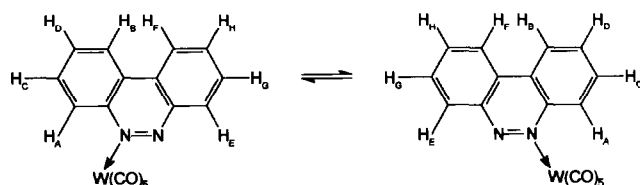


Fig. 2. Interconverting structures of $[\text{W}(\text{CO})_5(\text{bzc})]$ showing the hydrogen labelling.

complex where the formation of the $\text{N}^2 \rightarrow \text{W}$ bonded complex is greatly hindered by the close proximity of the methyl group. The solution populations of all com-

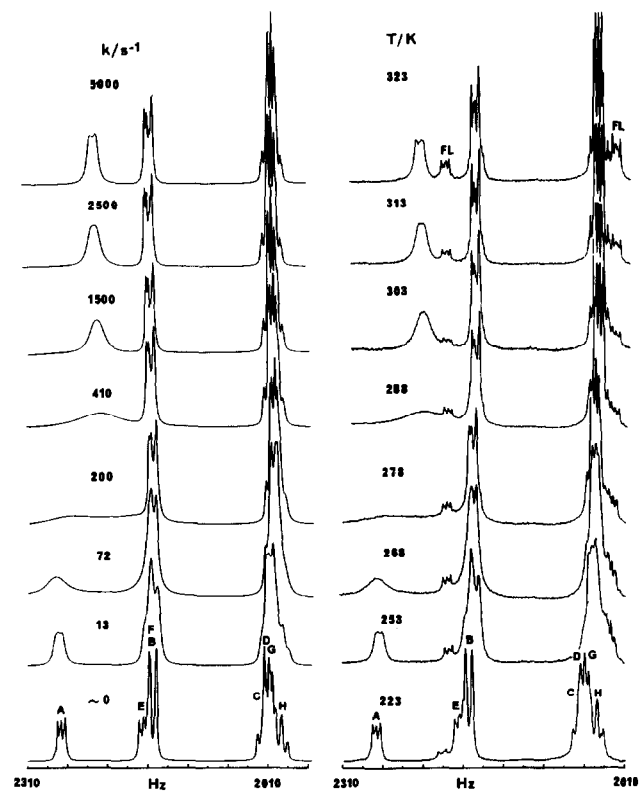


Fig. 3. Variable temperature ^1H spectra of $[\text{W}(\text{CO})_5(\text{bzc})]$ with computer simulated bandshapes (left) for the optimum rate constants for the 1,2-shift process. See Fig. 2 for hydrogen labelling. FL, free ligand.

TABLE 3. Activation parameters for the 1,2-metallotropic shift in the complexes $[\text{W}(\text{CO})_5(\text{bzc})]$, $[\text{Rh}(\text{CO})_2\text{Cl}(\text{bzc})]$ and $[\text{W}(\text{CO})_5\text{L}]$ (L = pydz, 3-Mepyzd, and 4-Mepyzd)

Complex	ΔH^\ddagger (kJ mol ⁻¹)	ΔS^\ddagger (J K ⁻¹ mol ⁻¹)	ΔG^\ddagger (298 K) (kJ mol ⁻¹)
$[\text{W}(\text{CO})_5(\text{bzc})]$	54.4 ± 0.9	-5.8 ± 3.1	56.1 ± 0.1
$[\text{cis-Rh}(\text{CO})_2\text{Cl}(\text{bzc})]$	62.5 ± 3.9	7 ± 13	60.4 ± 0.1
$[\text{W}(\text{CO})_5(\text{pydz})]$	84.7 ± 2.1	26 ± 7	77.1 ± 0.1
$[\text{W}(\text{CO})_5(3\text{-Mepyzd})]$	93.7 ± 2.6^a	58 ± 9^a	76.4 ± 0.1^a
	93.7 ± 2.5^b	95 ± 9^b	65.3 ± 0.1^b
$[\text{W}(\text{CO})_5(4\text{-Mepyzd})]$	98.1 ± 2.6^a	68 ± 9^a	77.9 ± 0.1^a
	98.1 ± 2.8^b	70 ± 9^b	77.4 ± 0.1^b

^a Major \rightarrow minor species. ^b Minor \rightarrow major species.

plex species are given in Fig. 4 and the ¹H NMR parameters characterizing the free ligands and their $\text{W}(\text{CO})_5$ complexes are contained in Table 4.

Certain trends in these data are worthy of note. The tungsten pentacarbonyl moiety induces significant coordination shifts ($\Delta\delta = 0.3\text{--}0.5$) in the *ortho* ring hydrogens A (or F), and smaller higher frequency shifts in the *meta* and *para* hydrogens C (or H) and D (or G) ($\Delta\delta = 0.1\text{--}0.2$). The effect on the hydrogens adjacent to the uncoordinated nitrogen B (or E) is less well defined. The methyl protons also experience high frequency shifts ($\Delta\delta \sim 0.1$). The other effect of metal coordination is to enhance the three-bond coupling ³J_{AC} of the *ortho* hydrogen to its neighbouring proton by ca. 0.5 Hz and to reduce the four-bond coupling, ⁴J_{AD}, by ca. 0.4 Hz. The other scalar couplings are not affected significantly.

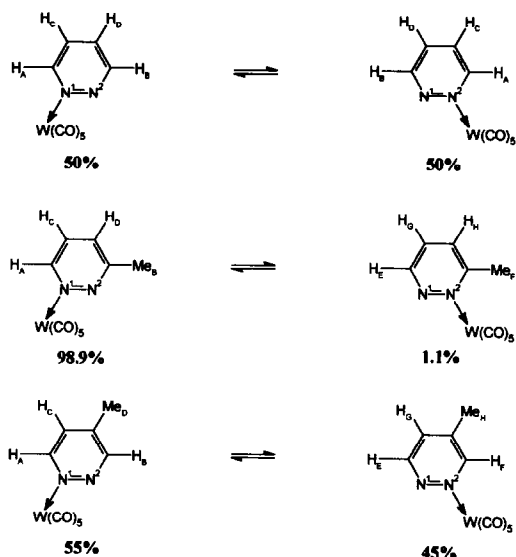


Fig. 4. Interconverting structures of the complexes $[\text{W}(\text{CO})_5\text{L}]$ (L = pydz, 3-Mepyzd, 4-Mepyzd) showing the hydrogen labelling and the percentage populations in CDCl_3 solution.

3.3. $[\text{W}(\text{CO})_5(\text{pydz})]$

The room temperature spectrum of this complex consisted of four chemical shifts, two of which were rather similar. The resulting ABCD pattern of lines was analysed iteratively using the LAOCN3 program [19] giving the parameters in Table 4.

Variable temperature spectra were recorded at temperatures between ambient and 110°C. Exchange broadening occurred between hydrogens A and B, with coalescence being achieved at 110°C. However, by this

TABLE 4. NMR data for pydz, 3-Mepyzd, 4-Mepyzd and their $\text{W}(\text{CO})_5$ complexes

Compound	Temperature (°C)	Aromatic or methyl hydrogen shifts, δ^a							
		A	B	C	D	E	F	G	H
pydz	21	8.94	8.94	7.29	7.29	—	—	—	—
$[\text{W}(\text{CO})_5(\text{pydz})]$	30	9.46	8.98	7.35	7.51	—	—	—	—
3-Mepyzd	30	8.91	2.59	7.27	7.23	—	—	—	—
$[\text{W}(\text{CO})_5(3\text{-Mepyzd})]$	30	9.29	2.70	7.38	7.42	^b	2.90	^b	^b
4-Mepyzd	30	8.92	8.94	7.22	2.29	—	—	—	—
$[\text{W}(\text{CO})_5(4\text{-Mepyzd})]$	30	9.26	8.81	7.30	2.42	8.80	9.30	7.37	2.40

		Scalar coupling constants, J (Hz)					
		AB	AC	AD	BC	BD	CD
pydz ^d	18	1.5	5.1	1.9	1.9	5.1	8.3
$[\text{W}(\text{CO})_5(\text{pydz})]$	30	1.3	5.6	1.5	2.0	5.1	8.3
3-Mepyzd	30	~ 0	4.9	1.7	~ 0	0.9	8.6
$[\text{W}(\text{CO})_5(3\text{-Mepyzd})]$	30	~ 0	5.4	1.2	~ 0	~ 0	8.5
4-Mepyzd	30	1.2	5.2	~ 0	2.4	~ 0.5	0.9
$[\text{W}(\text{CO})_5(4\text{-Mepyzd})]$	30	1.2	5.8	~ 0	2.5	~ 0.5	0.9
		1.2 °(EF)	5.1 °(EG)	~ 0 °(EH)	2.0 °(FG)	~ 0.5 °(FH)	0.9 °(GH)

^a Shifts measured in CDCl_3 rel. to int. Me_4Si . See Fig. 4 for labelling. ^b Signals too weak for detection. ^c Values refer to the less abundant solution complex. ^d Data in agreement with ref. 20.

temperature, any bandshape analysis was precluded by considerable decomposition of the complex. Instead, the 2D-EXSY technique [11] was employed, since this enabled exchange information to be extracted in the lower temperature range 19–50°C. Five 2D-EXSY spectra of the A and B hydrogens were recorded with mixing times varying between 2.5 and 0.1 s. Diagonal and cross-peak signal intensities were measured accurately and exchange rates in the range 0.096 to 3.22 s⁻¹ were calculated using the D2DNMR program [20]. These values provided the Eyring activation parameters shown in Table 3.

3.4. [W(CO)₅(3-Mepyzd)]

The ¹H spectrum of the complex recorded at 283 K revealed strongly coupled aromatic hydrogen signals and a methyl signal at δ = 2.70. The aromatic region was analysed iteratively [19] to give the data in Table 4. On close examination of the methyl region, a very weak signal was observed at δ = 2.90. This had comparable intensity to the ¹³C satellite signals of the intense methyl signal, and was attributed to the methyl hydrogens of the N² → W(CO)₅ complex. A search was made for correspondingly weak signals in the aromatic region but none were identified with any certainty. The weak signal in the methyl region was confirmed as being due to the other linkage isomer since on warming it showed exchange broadening with the major methyl signal. This broadening was carefully studied by total bandshape analysis (including the ¹³C satellites). Spectra were recorded up to a temperature of 60°C, and fit-

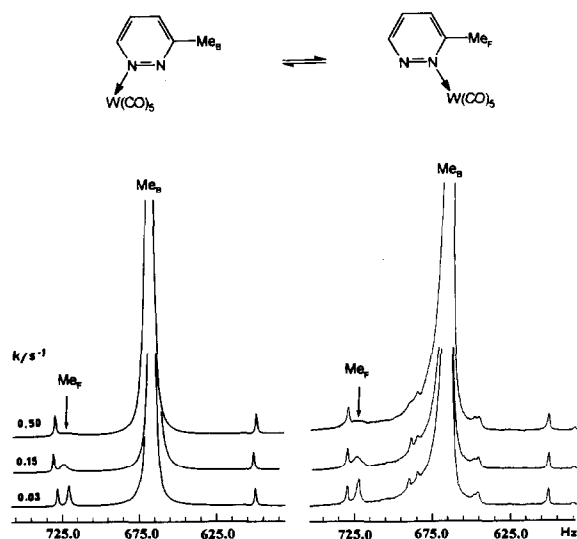


Fig. 5. Experimental and computer simulated ¹H spectra of the methyl signals of [W(CO)₅(3-Mepyzd)] in CDCl₃ at various temperatures. Carbon-13 satellite signals are shown in both experimental and simulated spectra.

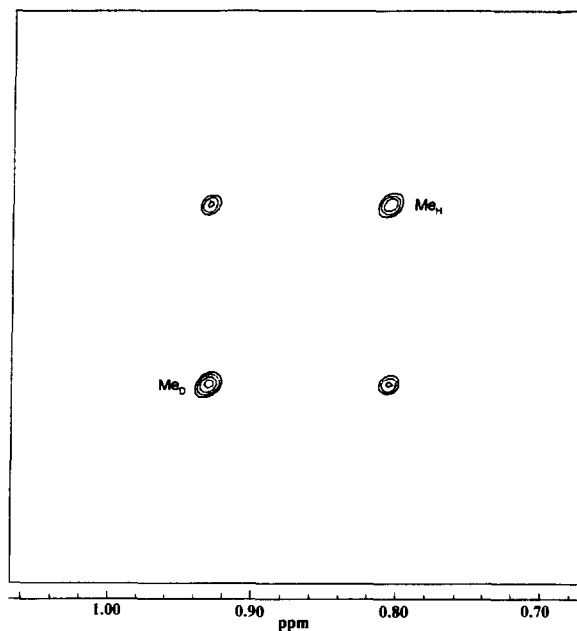


Fig. 6. ¹H 2D-EXSY NMR spectrum of [W(CO)₅(4-Mepyzd)] in C₆D₆ at 30°C (methyl region only). Mixing time was 1.5 s.

tings made on seven spectra in the range 10–50°C. Despite the fact that the weak methyl signal broadened beyond detection above 30°C, satisfactory fittings of total methyl spectra were achieved (Fig. 5). Rate constants, for major → minor isomer exchanges, were in the range 0.03–5.0 s⁻¹. Such magnitudes are exceptionally low for NMR bandshape analyses and are due to the general theoretical prediction that when exchange occurs between two very unequally populated sites, the nuclei in the sparsely populated site will be highly sensitive to the rate process [10]. This follows from the equilibrium expression relating forward (k_{12}) and reverse (k_{21}) rate constants and site populations (p_1 , p_2), namely $p_1 k_{12} = p_2 k_{21}$. In the present case, $p_1/p_2 = 98.9\%/1.1\% (= 89.9)$, so that $k_{21} = 89.9 k_{12}$, and thus the weak signal will display appreciable line broadening for extremely small values of k_{12} . Temperature dependences of both k_{12} and k_{21} gave the activation parameters in Table 3.

3.5. W(CO)₅(4-Mepyzd)]

In this complex, the methyl group in the 4-position of the pyridazine ring exerts only a minor influence on the preferred linkage isomer of the W(CO)₅ complex, and both forms exist in CDCl₃ (or C₆D₆) solution, in

TABLE 5. Rate data for the 1,2-metallotropic shift in $[\text{W}(\text{CO})_5(4\text{-Mepyz})]$ in C_6D_6 solvent

Temperature (°C)	Technique	Mixing time τ_m (s)	k_{12}^a (s^{-1})
19	2D-EXSY	2.5	0.060
30	2D-EXSY	1.5	0.305
40	2D-EXSY	0.7	0.987
45	2D-EXSY	0.2	1.795
50	2D-EXSY	0.1	3.11
50	1D-BSA	–	2.8
60	1D-BSA	–	12.0

^a More abundant \rightarrow less abundant species.

the ratio 55%/45%, the more abundant species being the N^1 bonded complex. The 1,2-shift is effectively arrested on the 1D NMR time scale at 19°C and the spectrum is straightforwardly analysed on a first-order basis (see Table 4 for static parameters). ^1H spectra were then recorded up to a temperature of 80°C in C_6D_6 . Some exchange broadening was observed in the signals above *ca.* 40°C but this was accompanied by considerable decomposition of the complex above 60°C preventing any bandshape analysis. It was therefore decided to use the 2D-EXSY method to extract the rate information in a lower temperature range, namely 19–50°C, and to supplement this with bandshape analysis data taken from 1D spectra at 50°C and 60°C. The methyl regions of the spectra were chosen for both the 1D and 2D techniques and C_6D_6 was the chosen solvent since it produced a larger chemical shift distinction between the methyls ($\Delta\delta = 0.12$) than the CDCl_3 solvent. A typical 2D-EXSY spectrum of the methyl signals, D and H, and their associated cross-peaks is shown in Fig. 6. The rate data extracted using both techniques are presented in Table 5. Both data sets fitted the same linear Eyring plot ($\ln(k/T)$ versus $1/T$) and produced the activation energy data in Table 3.

4. Discussion

There are two main discussion points to be addressed, namely the factors governing the activation energies of these 1,2-haptotropic shifts and the nature of the transition state intermediate.

From Table 3, it is strikingly apparent that the 1,2-shift occurs far more readily in the case of the benzo[*c*]cinnoline complexes than in the pyridazine complexes, the difference in ΔG^\ddagger values for the two series being of the order of 20 kJ mol^{-1} . In the benzo[*c*]cinnoline case, there is also some clear metal dependence of the activation energy with $\text{Rh} > \text{W}$, but the change in coordination geometry from square planar Rh to octahedral W may also be a contributing

factor. The activation energy values (ΔG^\ddagger) for the pyridazine complexes are virtually independent of methyl substitution on the ring and occur in the narrow range 76–78 kJ mol^{-1} . Such a range includes the value of 77.4 kJ mol^{-1} obtained previously [7] for the phthalazine complex $[\text{W}(\text{CO})_5(\text{phth})]$. This implies that the exceptionally low energy value for $[\text{W}(\text{CO})_5(\text{bzc})]$ is associated with the different fused ring geometry of the bzc ligand. In the latter, the hydrogens adjacent to the nitrogens (H_A and H_E in Fig. 2) are directed more towards the nitrogen lone pairs than in phthalazine or pyridazine. The lone pairs are thus likely to be oriented somewhat towards each other, so that when the metal moiety is attached, the ground state structure of this complex becomes distorted towards the geometry of the transition state (*vide infra*) and a lower activation energy for the 1,2-shift will ensue. Experimental support for this postulate may be obtained from the recent X-ray crystal structure of $[\text{W}(\text{CO})_5(\text{bzc})]$ where the angles W-N-C and W-N-N are reported to be 128.9(6)° and 110.5(5)°, respectively [21].

In the case of the pyridazine complexes, the N lone pair orientations are not influenced by any internal ligand interactions and the spatial movement of the 1,2-shift will be significantly greater than in the benzo[*c*]cinnoline case.

Such generalizations, namely that the energy barrier for these 1,2-shifts is dependent on the nitrogen–nitrogen separation and the lone pair orientations are in full accord with some extended Hückel calculations by Alvarez *et al.* [22] on the preferred pathway for this fluxional process. They conclude that the intermediate structure will be a bound bidentate, 20-electron species. The chosen pathway is considered to be one in which sliding and rotation of the ligand are combined to make the M–N distances in the intermediate equal to the bonding distance in the monodentate case. The geometry of the transition state has been evaluated more closely by Kang *et al.* [23]. They studied the interaction of $\text{Cr}(\text{CO})_5$ with a variety of diazenes, including pyridazine, using extended Hückel calculations, which, in one case, were checked at the *ab initio* level. They concluded that for the $\text{Cr}(\text{CO})_5$ complexes of pyridazine and naphthyridine, the transition states were characterized by very long Cr–N bonds, in other words they possess substantial dissociative character, in contrast to complexes of *cis* and *trans* N_2H_2 where a π -bonded intermediate appears to be favoured.

Our calculations of activation entropies for the 1,2-shifts in the $\text{W}(\text{CO})_5$ complexes of pyridazine and its methyl substituted derivatives lend support to this proposal, since in all three complexes the ΔS^\ddagger values are significantly positive, indicative of intermediates with a degree of dissociative character. In contrast, our ΔS^\ddagger

data for the benzo[*c*]cinnoline complexes are approximately zero, suggesting that these intermediates are non-dissociative, being either π -bonded complexes or bidentate, 20-electron species. Unfortunately, theoretical calculations on $[M(CO)_5(bzc)]$ complexes have not been made so that it is not possible to give a firm preference to these alternative structures but the π -bonded intermediate would seem more likely on chemical grounds. Activation entropies are notoriously difficult to measure reliably by DNMR techniques [10] so some caution must be attached to these conclusions. However, the quality of the bandshape analysis and 2D-EXSY NMR fittings of these complexes provide confidence in attaching real chemical significance to these data.

References

- 1 M.N. Ackermann, R.M. Willett, M.H. Englert, C.R. Barton and D.B. Shewitz, *J. Organomet. Chem.*, **175** (1979) 205.
- 2 M.N. Ackermann, D.B. Shewitz and C.R. Barton, *J. Organomet. Chem.*, **125** (1977) C33.
- 3 C.C. Frazier, III and H. Kisch, *Inorg. Chem.*, **17** (1978) 2736.
- 4 M. Herberhold and K. Leonhard, *Angew. Chem., Int. Ed. Engl.*, **15** (1976) 230.
- 5 M. Herberhold, K. Leonhard and C.G. Kreiter, *Chem. Ber.*, **107** (1974) 3222.
- 6 K.R. Dixon, *Inorg. Chem.*, **16** (1977) 2618.
- 7 K.R. Dixon, D.J. Eadie and S.R. Stobart, *Inorg. Chem.*, **21** (1982) 4318.
- 8 T.E. Reed and D.G. Hendricker, *J. Coord. Chem.*, **2** (1972) 83.
- 9 M. Kooti and J.F. Nixon, *J. Organomet. Chem.*, **105** (1976) 217.
- 10 J. Sandström, *Dynamic NMR Spectroscopy*, Academic Press, London, 1982.
- 11 K.G. Orrell, V. Šik and D. Stephenson, *Prog. NMR Spectrosc.*, **22** (1990) 141.
- 12 D.F. Shriver, *Manipulation of Air-Sensitive Compounds*, McGraw-Hill, New York, 1969.
- 13 D.A. Kleier and G. Binsch, *DNMR3 Program 165*, Quantum Chemistry Program Exchange, Indiana University, USA, 1970.
- 14 E.W. Abel, T.P.J. Coston, K.G. Orrell, V. Šik and D. Stephenson, *J. Magn. Reson.*, **70** (1986) 34.
- 15 T.E. MacKenzie, Ph. D. Thesis, University of Exeter, 1983.
- 16 C. Bessenbacher and W. Kaim, *J. Organomet. Chem.*, **369** (1989) 83.
- 17 J.B. Brandon, M. Collins and K.R. Dixon, *Can. J. Chem.*, **56** (1978) 950.
- 18 J.F. Nixon and M. Kooti, *J. Organomet. Chem.*, **149** (1978) 71.
- 19 A.A. Bothner-By and S.M. Castellano, in D.F. De Tar (ed), *Computer Programs for Chemistry*, Vol. 1, W.A. Benjamin, New York, 1968.
- 20 V.M.S. Gil and J.L. Pinto, *Mol. Phys.*, **16** (1969) 623; **19** (1970) 573.
- 21 E.K. Pham and L. McElwee-White, *Acta Crystallogr. Sect. C*, **48** (1992) 1120.
- 22 S. Alvarez, M-J. Bermejo and J. Vinaixa, *J. Am. Chem. Soc.*, **109** (1987) 5316.
- 23 S-K. Kang, T.A. Albright and C. Mealli, *Inorg. Chem.*, **26** (1987) 3158.